JOURNAL OF GEOPHYSICAL RESEARCH, VOL. 85, NO. C4, PAGES 1910–1916, APRIL 20, 1980

# The Batchelor Spectrum and Dissipation in the Upper Ocean

THOMAS M. DILLON AND DOUGLAS R. CALDWELL

*School of Oceanography, Oregon State University, Corvallis, Oregon 97331*

Observations of vertical temperature microstructure at ocean station P during the mixed layer experiment (Mile) indicate that the shape of the high-frequency temperature gradient spectrum depends on the relative strengths of turbulence and stratification. For low Cox number $\langle(dT/dz)^2\rangle/\langle dT/dz\rangle^2$ the linear range of the Batchelor spectrum is not well approximated by observed spectra, while for high Cox number a remarkably close correspondence to the Batchelor spectrum is found. Dissipation rates calculated by the temperature gradient spectrum cutoff wave number method show a dramatic contrast in turbulence between low and high wind speed periods separated by only 3 hours, showing that the response of the mixed layer and transition zone to wind forcing is rapid. Some indication is found that the thermocline may also respond rapidly to surface forcing.

## INTRODUCTION

Numerous comparisons of the theoretical universal temperature and temperature gradient forms predicted by *Batchelor* [1959] have been made with spectra measured in natural waters [e.g., *Grant et al.*, 1968; *Gregg*, 1976, 1977; *Nasmyth*, 1970; *Elliot and Oakey*, 1976; *Marmorino and Caldwell*, 1978]. While such measurements often compare favorably with the viscous-convective Batchelor spectrum by showing a linear range, it has seldom been possible to resolve the entire temperature gradient spectrum for a variety of reasons, including limited or unknown sensor frequency response characteristics and too much noise. When the spectrum has been resolved beyond the microstructure peak, a detailed comparison with the Batchelor spectrum has not proved favorable in certain cases [*Nasmyth*, 1970; *Elliot and Oakey*, 1976], prompting at least one investigator [*Elliot and Oakey*, 1976] to propose a different model for the high-frequency spectrum. Since the applicability of a Batchelor spectrum allows one to make an estimate of the kinetic energy dissipation rate from a temperature spectrum alone, it is important that the nature of the viscous-convective spectrum be well understood and that the universality of the Batchelor spectrum in stratified fluids be tested.

A companion paper describes a test of the hypothesis that the cutoff wave number in the spectrum is identifiable with the Batchelor wave number [*Caldwell et al.*, 1980]. The result is favorable when turbulent fluctuations are weak in comparison to the mean stratification, but because it assumes strong stratification, the test is not relevant to intense turbulence. The present paper shows that the Batchelor spectral form is followed more closely when the fluctuations are strong. It is thus plausible that the cutoff wave number is related to the Batchelor wave number in both cases and so can be used to estimate dissipation. The definitive test of the relation between the cutoff wave number and the dissipation will be direct simultaneous measures of the smallest scales of both velocity and temperature. This difficult task has not yet been accomplished, and so the present paper and its companion must be assessed as indirect evidence only, showing that the relations between the cutoff wave number, Batchelor scale, and dissipation rate are plausible and consistent.

During the Mile experiment at ocean station P (50°N, 145°W), August–September 1977, we performed a number of casts with a vertical microstructure profiling device in the surface layer and seasonal thermocline during a moderate storm and found that the temperature gradient spectrum was almost always resolved to an easily identifiable cutoff. With this data set a test can be made of the universality of the Batchelor spectrum in natural stratified waters.

In addition, the particular meteorological conditions encountered during the microstructure casts on Julian date 244 at station P enable us to use the Batchelor scaling to address questions pertinent to mixed layer dynamics: (1) What is the time scale of response of the surface waters to surface forcing? (2) How is dissipation distributed vertically, and does the distribution vary as surface conditions change? (3) Can the vertical distribution of dissipation be associated with features of the stratification? (4) Does the upper seasonal thermocline respond significantly to surface forcing?

## THEORETICAL BACKGROUND

The Batchelor spectrum of temperature gradient fluctuations in one dimension may be written [*Gibson and Schwarz*, 1963]

$$S(k) = (q/2)^{1/2}\chi_\theta k_B^{-1} D^{-1} f(\alpha) \tag{1}$$

where $k$ is the wave number (here in units of radians per unit length), $q$ is a universal constant, $\chi_\theta$ is the temperature variance dissipation rate satisfying

$$\chi_\theta = 6D\int_0^\infty S(k)\,dk = 6D\left\langle\left(\frac{\partial T'}{\partial z}\right)^2\right\rangle \tag{2}$$

$D$ is the molecular diffusivity, $T'$ is a temperature fluctuation, $z$ is depth, $k_B$ is the Batchelor wave number $(\epsilon\nu^{-1}D^{-2})^{1/4}$, $\epsilon$ is the kinetic energy dissipation rate, $\nu$ is the kinematic viscosity, and $\alpha$ is a nondimensional wave number $kk_B^{-1}(2q)^{1/2}$. The nondimensional shape of the spectrum is given by

$$f(\alpha) = \alpha\left\{e^{-\alpha^2/2} - \alpha\int_\alpha^\infty e^{-x^2/2}\,dx\right\} \tag{3}$$

If an inertial subrange exists, the transition from inertial to viscous-convective behavior occurs at the wave number $k_* \equiv C_* Pr^{-1/2}k_B$, and for wave numbers in the equilibrium range smaller than $k_*$ the spectrum is given by

$$S(k) = \beta\chi_\theta\epsilon^{-1/3}k^{1/3} \tag{4}$$

Here both $C_*$ and $\beta$ are universal constants, and $Pr$ is the Prandtl number $\nu/D$.

Copyright © 1980 by the American Geophysical Union.

Paper number 9C1648.
0148-0227/80/009C-1648$01.00

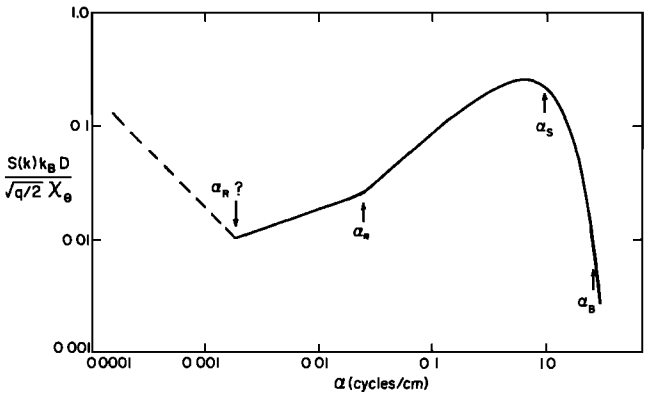


Fig. 1. Nondimensional universal spectrum with a 'fine structure' range for $\alpha < \alpha_R$, the Richardson wave number; an inertial subrange for $\alpha_R < \alpha < \alpha_*$; and a viscous-convective Batchelor spectrum for $\alpha > \alpha_*$. The positions of the Kolmogorov wave number $\alpha_s$ and Batchelor wave number $\alpha_B$ are determined by choice of the universal constant $q$ ($2(3)^{1/2}$ assumed here), while the shape of the spectrum for $\alpha > \alpha_*$ is independent of universal constants. The inertial subrange is rarely observed in vertical microstructure.

Nondimensionalizing the spectrum by the Batchelor scale $k_B$ and $\chi_\theta$ yields the equilibrium range spectrum (Figure 1)

$$S(k)\left\{(q/2)^{1/2}\frac{\chi_\theta}{k_B D}\right\}^{-1} = f(\alpha) \qquad \alpha \geq \alpha_* \tag{5}$$

$$S(k)\left\{(q/2)^{1/2}\frac{\chi_\theta}{k_B D}\right\}^{-1} = 2^{1/3}Pr^{-1/3}\beta q^{-2/3}\alpha^{1/3} \qquad \alpha_R < \alpha < \alpha_*$$

where $\alpha_* = C_* Pr^{-1/2}(2q)^{1/2}$ and $\alpha_R$ marks the wave number at which the fine structure and internal wave effects become appreciable. Continuity at $k_*$ establishes the relation between $q$, $\beta$, and $C_*$ as [*Williams and Paulson,* 1977]

$$\beta = qC_*^{2/3} \tag{6}$$

*Gibson* [1968] advanced a theoretical argument that $3^{1/2} < q < 2(3)^{1/2}$; *Grant et al.* [1968] estimated $q = 3.9 \pm 1.5$ and $C_* = 0.024 \pm 0.008$ (standard error estimates). *Williams and Paulson* [1977] found from inertial subrange measurements in air that $\beta \simeq 0.5$ and noted a small but definite dependence of $\beta$ upon Reynolds number. The atmospheric measurements of $\beta$ are surely more accurate than one could reasonably expect from marine measurements, and there is no reason to expect inertial subrange parameters such as $\beta$ to depend on Prandtl number. If $q$ is $2(3)^{1/2}$ and $\beta$ is 0.5, $C_*$ becomes 0.055, twice as large as the value found by *Grant et al.* [1968] and substantially larger than the values 0.03 and 0.04 found by *Gibson et al.,* [1970] but only half the value of 0.1 estimated by *Gibson and Schwarz* [1963] from laboratory measurements. There is thus a large uncertainty regarding the value of $C_*$.

If dissipation rates are to be estimated from the cutoff frequency of the Batchelor spectrum, $q$ is the only relevant universal constant. A percentage error in $q$ is reflected as a systematic error twice as large in $\epsilon$. This error may not be as large as that resulting from direct high-frequency velocity determinations of $\epsilon$ in water and will not affect relative measures of $\epsilon$, so that depth variability can be assessed without error from this source.

Although the Batchelor spectrum was proposed for homogeneous, locally isotropic turbulence in an unstratified fluid with large Prandtl number, it is clear, in contrast to inertial subrange turbulence, that the spectral form is not an asymptotic limit of high Reynolds number turbulence. *Batchelor* [1959] suggests that even when the Reynolds number is so small that an inertial subrange does not exist, the Batchelor form may be found.

The effect of stratification on the Batchelor spectrum, however, has not been explored. In natural waters (Prandtl number of the order of 10), temperature fluctuations are usually caused by turbulent stirring in the presence of a mean gradient. The level of turbulence relative to the stratification is likely to be important in determining the scale at which local isotropy is approached and in determining whether or not a Batchelor spectrum is found.

A measure of the turbulence relative to the stratification may be constructed in the form of a 'stratification Reynolds number' $R_s = Ulv^{-1}$, where $U$ is estimated as $\epsilon^{1/3}l^{1/3}$ [*Tennekes and Lumley,* 1972] and the length scale is estimated as the Richardson length $l = \epsilon^{1/2}N^{-3/2}$, where $N$ is the local buoyancy frequency. Thus $R_s$ reduces to $(\epsilon\nu^{-1})N^{-2}$, a squared ratio of time scales of the turbulence and stratification. If $\epsilon$ is estimated by the Cox number $Cx = \langle(dT'/dz)^2\rangle/\langle dT/dz\rangle^2$ and $N$ [*Caldwell et al.,* 1980], $\epsilon$ is proportional to $DN^2Cx$, so that $R_s$ is proportional to $Pr^{-1}Cx$. We might therefore expect that the approach to the Batchelor spectrum in a stratified natural fluid would depend on the Cox number.

We imagine that for small Cox number (turbulence weak compared to the stratification), small-scale temperature features which are possibly remnants of the mean stratification may exist at wave numbers large enough to coincide with wave numbers in the viscous-convective subrange and alter the low wave number portion of the Batchelor spectrum. A similar situation was hypothesized by *Gregg* [1977], who, upon examining spectra from the main oceanic thermocline, which somewhat resembled the Batchelor spectrum but failed to reveal a distinct linear range, supposed that the low wave number viscous-convective spectrum was 'contaminated' by the fine structure–internal wave spectrum.

In the remainder of this work, following a brief experimental description, we report that for large Cox number in the oceanic surface layer the Batchelor spectrum closely approximates observed spectra. For smaller Cox number the observed spectra depart significantly from the Batchelor form, showing a broader, less peaked shape. We then present depth profiles of dissipation calculated by the cutoff wave number technique and compare profiles taken during low and high winds.

## Experimental Description

The vertical microstructure profiles to be discussed here were collected at ocean station P during August–September 1977 as part of the Mile experiment. The microstructure profiler used was a small, winged, nearly freely falling device similar to that described by *Caldwell et al.* [1975]. The fall rate is adjustable; for these runs it was set at 10 cm $s^{-1}$. The probe carried two thermistors, a Neil Brown conductivity sensor, and a pressure sensor. The data were transmitted to the ship through a small-diameter (1.6 mm) cable containing four pairs of expendable bathythermograph (XBT) wire sheathed in a Kevlar strength member and coated with syntactic foam; the foam density is adjusted so that the entire cable has a slight tendency to sink.

One thermistor was redundantly amplified, and the two signals were sent to the surface through different wires, where it was again amplified, differentiated, filtered with a 12-pole Butterworth filter (3-dB frequency set at 30 Hz), and then digitized and recorded at a rate of 90 $s^{-1}$. Since most of the noise

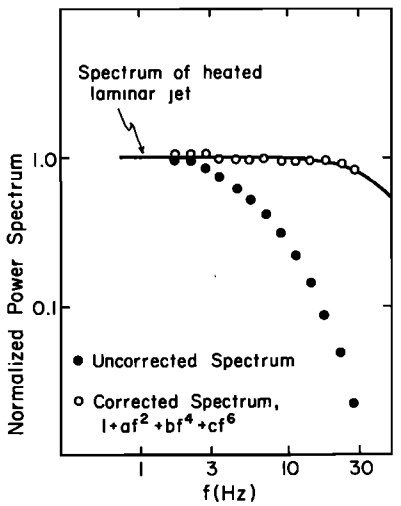


Fig. 2. Frequency response of the P-85 thermistor as determined by passing the thermistor through a heated laminar jet at 10 cm $s^{-1}$; $a = 2.6352 \times 10^{-2}$, $b = -2.1897 \times 10^{-5}$, and $c = 3.2556 \times 10^{-7}$.

content of the temperature signals originated in the first stage amplifier, these noise sources were incoherent on the two channels. A calculation of the in-phase power [*Caldwell et al.*, 1969] allowed a significant reduction in noise level to be made. A second thermistor was differentiated inside the probe rather than at the surface but otherwise preprocessed in a manner similar to the first. The conductivity was sent to the surface on the remaining XBT pair, and the pressure signal was transmitted in frequency-modulated form in the range 500–1300 Hz.

The frequency response of the thermistors (Thermometrics P-85) was determined by a test similar to the Fabula test [*Fabula*, 1968], using for the plume a laminar jet emitted from a 0.30 × 12.7 mm nozzle. The velocity of the jet was 2–3 cm $s^{-1}$ at the height where the probe, moving at 10 cm $s^{-1}$, passed through. A detailed map of the jet revealed a nearly Gaussian temperature distribution with a spectral power 3 dB in wavelength of 1.9 mm. The frequency response, which substantially agrees with a similar test performed by M. C. Gregg (personal communication, 1979) on another P-85, could not be well described by either single or double pole response functions; for computational purposes, a power series in even powers of frequency up to the sixth power was used instead. It describes the response to 30 Hz with 3% standard error (Figure 2).

The data were collected on Julian date 244, 1977, between the hours 0500 and 1200 UT in the midst of a moderate storm (maximum sustained wind speeds of 16 m $s^{-1}$). This was the second storm encountered during the Mile experiment. The low-pressure center of the storm passed directly over station P, and a dramatic change in wind speed (Figure 3) was noted, along with a reversal of wind direction, at 0200 hours. Casts during the earlier part of the sampling period, when winds were low, show markedly less activity in the surface layer and thermocline than later casts in higher winds [*Dillon and Caldwell*, 1977], showing a rapid response of the upper waters to increasing wind stress. We sampled, in a short period of time, water with greatly different levels of turbulence relative to the mean stratification.

## Computational Techniques

A nondimensional form of the high-frequency gradient spectrum may be determined if both $\chi_\theta$ and $\epsilon$ are known. If the observed spectrum is well resolved, $\chi_\theta$ may be found by integrating the spectrum. Without simultaneous high-frequency velocity measurements, $\epsilon$ cannot be measured directly. An estimate of the dissipation rate can be made from the spectrum if the transitional wave number $k_*$ can be determined. This technique is of limited applicability, however, because spectra exhibiting unambiguous transitions from the inertial to the viscous-convective subrange are found in only a few of the casts. We believe that this is so because the low wave numbers of the inertial subrange spectrum can be seen only in thick sections of the water column. The turbulence properties in such a thick section may change with depth, causing the observed spectrum to be nonstationary. These low wave numbers may also be contaminated by the fine structure–internal wave spectrum [*Gregg*, 1977].

If the entire spectrum has been resolved, a high wave number normalization can be used. Suppose that the fluid is turbulent and the signal is well above noise. Then the gradient spectrum will exhibit a peak of some sort followed by a very rapid roll-off. First, we calculate $\chi_\theta$ by integration; then we define a cutoff wave number $k_c$ as the wave number at which the spectrum falls to some fraction, say, one tenth, of its peak value. If the Batchelor spectrum does obtain, $k_B$ will be some fraction (which depends on the value of $q$ assumed) of $k_c$. Wave numbers are then nondimensionalized by $k_B^{-1}(2q)^{1/2}$, and the spectrum $S(k)$ is nondimensionalized by $(q/2)^{1/2}\chi_\theta k_B^{-1} D^{-1}$. Note that while the particular value of $k_B$ (and also $\epsilon_B = k_B^4 \nu^{-1} D^{-1}$) depends on $q$, the shape of the nondimensionalized spectrum is independent of $q$. A number of such nondimensionalized spectra may then be ensemble-averaged and compared to the Batchelor spectrum. This comparison will be independent of the particular value used for $q$.

A slightly improved technique is to find the cutoff wave number $k_c$ (and hence $k_B$ and $\epsilon_B$) by performing a nonlinear weighted least squares fit to the Batchelor spectrum. The weighting used corresponds to the degrees of freedom of the band-averaged spectral estimates [*Otnes and Enochson*, 1972]; hence the high-frequency roll-off portion of the spectrum is much more heavily weighted (by a factor of 25–50) than the lower-frequency, prepeak linear region of the spectrum. In

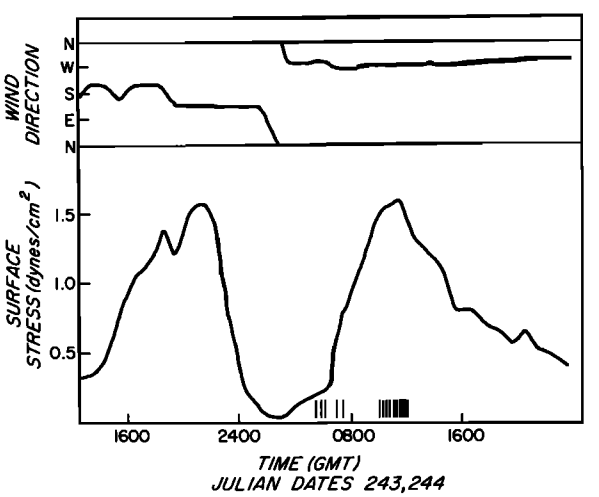


Fig. 3. Surface stress and wind direction during the second significant storm encountered during the Mile experiment. Wind speed dropped to near zero, and wind direction changed as the low-pressure storm center passed over station P. Times of the five microstructure drops during light winds and the 10 drops during storm winds are indicated as vertical bars on the lower portion of the figure.

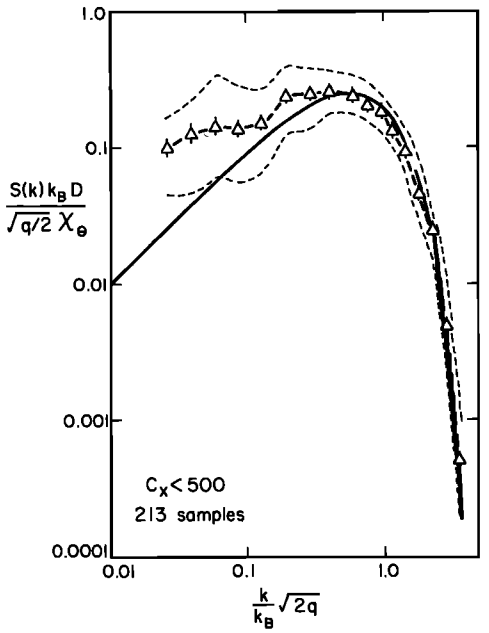


Fig. 4. Ensemble-averaged nondimensional spectrum for Cox numbers less than 500. The lower wave number portion of the spectrum departs significantly from the Batchelor spectrum (solid curve). Error bars are the standard error of the mean based on the standard deviation. The dashed envelope shows the average positive and negative deviation from the mean; that is, half of the spectral estimates lie within the envelope. Thus although the mean of the spectral values has a small uncertainty (the bars), the estimates in an individual spectrum may lie quite far from the mean.

addition, since the spectrum rolls off so rapidly, the fitting procedure will be very sensitive to the slope of the spectrum in the cutoff range of wave numbers and insensitive to the spectral estimates at low, prepeak wave numbers.

After performing the high-frequency normalization and ensemble averaging groups of spectra we will know that we have found a Batchelor form if the low wave number region of the ensemble average agrees with the linear region of the Batchelor spectrum. The high wave number roll-off region is constrained by the fit to follow the Batchelor spectrum as well as it may, but the low wavenumber region is not.

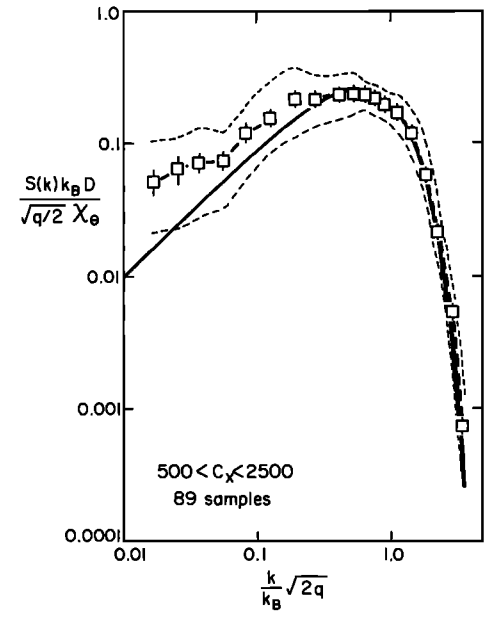


Fig. 5. Ensemble-averaged nondimensional spectrum for intermediate Cox numbers. The low wave number portion of the spectrum is closer to the Batchelor spectrum than the low Cox number spectrum but still is significantly different. Thus although the mean of the spectral values has a small uncertainty (the bars), the estimates in an individual spectrum may lie quite far from the mean.

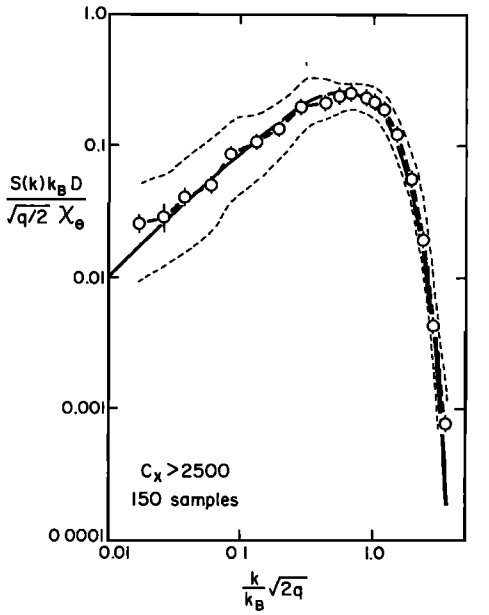


Fig. 6. Ensemble-averaged nondimensional spectrum for large Cox numbers. The low wave number portion of the spectrum is in remarkably close agreement with the Batchelor spectrum. Thus although the mean of the spectral values has a small uncertainty (the bars), the estimates in an individual spectrum may lie quite far from the mean.

To minimize vertical intermittency, the data were broken into 512 point segments (~60 cm). (Even for these thin samples, however, there is no guarantee that the turbulence is homogeneous throughout the segment.) A Gaussian window was applied to each segment to reduce spectral leakage, and a fast Fourier transform was applied. After band averaging, the spectral estimates were corrected for thermistor attenuation. Only fully resolved spectra are included in this paper; a spectrum was operationally defined as 'resolved' if it fell to 10% of its peak value and was still above noise levels before the 3-dB frequency (30 Hz) of the analogue filter was reached. Approximately 90% of the spectra in the surface layer met this criterion.

## SPECTRAL SHAPES

Nondimensional spectra from all surface layer runs on Julian day 244 were grouped together in ranges of Cox number for comparison to the Batchelor form (the surface layer was defined as the region of temperature within 0.25° C of the surface value). Spectra with low Cox numbers were markedly different from those with a high Cox number. The low $Cx$ spectra ($Cx < 500$) characteristically exhibit a broad maximum before roll-off and do not agree well with the Batchelor form in the linear range (Figure 4). Spectra with higher values of $Cx$ progressively approach the Batchelor spectrum at low wave number (Figure 5), and for $Cx > 2500$ the low-frequency fit to the Batchelor form is quite remarkable (Figure 6).

The same trend of the averaged spectra to approach the Batchelor spectrum is found if they are grouped by $R_s$ =

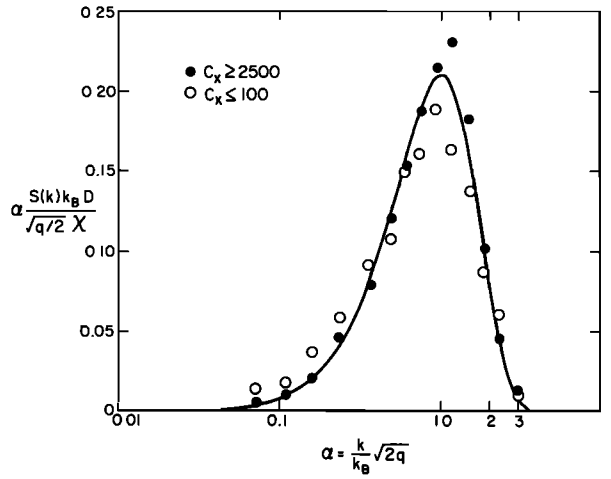


Fig. 7. Variance-preserving plot of ensemble-averaged nondimensional spectra for large (solid circles) and small (open circles) Cox numbers compared to the Batchelor spectrum (solid curve). Slightly elevated values of the large Cox number spectrum near the peak may indicate violation of Taylor's hypothesis.

$\epsilon_B \nu^{-1} N^{-2}$. Similar behavior is exhibited when the spectra are classified and averaged in terms of cutoff wave number or buoyancy frequency; that is, low $k_c$ and high $N$ spectra are broad and flat, while high $k_c$ and low $N$ spectra resemble the Batchelor spectrum, although the approach to the Batchelor form is less pronounced for these classifications than for classification by $Cx$ or $R_\rho$.

We have at present no means of knowing whether the broad spectra seen at low Cox number are indicative of small-scale temperature structures attributable to the 'mean' stratification or whether they have a fundamental meaning for turbulence in a stratified fluid. Although one might claim that all temperature fluctuations are in a sense due to a turbulent field, a clear distinction can be made between stratified turbulent fields in which the temperature gradient spectrum depends only on $\chi_\theta$ and $\epsilon_B$ and those in which it depends on additional parameters ($Cx$, for example). In the former case, fluctuations in the viscous-convective subrange will not depend on the history of the fluid but simply reflect the state of the local dissipation. In the latter case the mean stratification, which certainly depends on the history of the fluid, seems to be important (in a way not yet clearly defined). Until we have evidence to show otherwise, we assume that although the stratification may be important in the viscous-convective subrange at low wave numbers in the prepeak region, the wave number of the spectral roll-off depends only on the local dissipation rate; that is, the highest-frequency turbulence is independent of stratification. The effect of stratification is simply to add a mean 'background' spectrum at low viscous-convective wave numbers, as was suggested by *Gregg* [1977]. This point of view has some empirical backing, since the dissipation rate calculated from the cutoff wave number is highly correlated with the dissipation rate as calculated from $N$, $D$, and $Cx$ [*Caldwell et al.*, 1980].

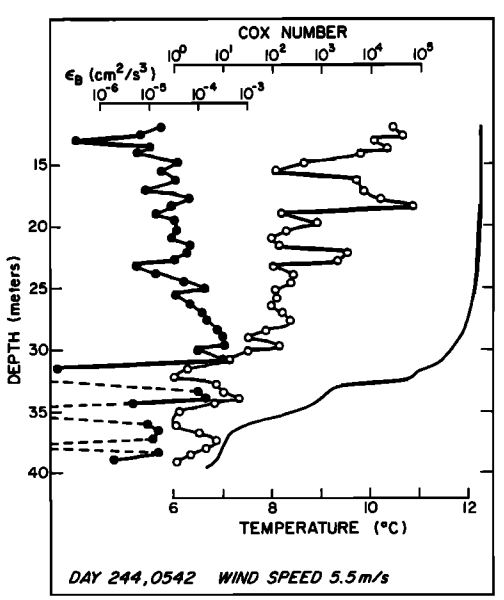


Fig. 8. Profiles of $\epsilon_B$, Cox number, and temperature during light winds. Note the intermittency in $\epsilon_B$ and Cox number and a trend toward increasing $\epsilon_B$ as the seasonal thermocline is approached. The dashed line indicates a region where the spectrum was unresolved. Estimates of Cox number in the surface layer may be particularly uncertain because of the small temperature gradient.

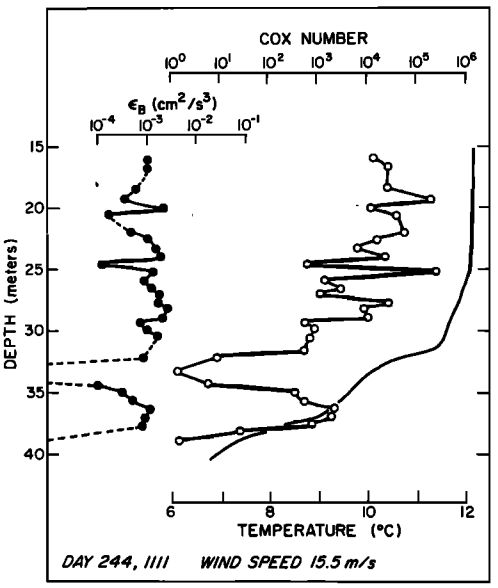


Fig. 9. Profiles of $\epsilon_B$, Cox number, and temperature during strong winds. No systematic trend is seen in $\epsilon_B$. Note the vertical intermittency in $\epsilon_B$ in the thermocline below 32 m.

Stratified regions may exhibit 'fossil turbulence' [*Turner*, 1973], that is, temperature microstructure persisting after velocity gradients have disappeared. *Schedvin* [1979] states that when $(\epsilon_B/\nu)^{1/2} \leq N$, the microstructure may be fossil. If $\epsilon_B$ can be approximated as $N^2DCx$ [*Caldwell et al.*, 1980], this condition for fossilization is equivalent to $Cx < Pr$, a condition rarely seen in the actively mixing surface layer. For the data examined here, $(\epsilon_B/\nu)^{1/2}$ was less than $N$ only 6% of the time, and these cases were confined to the thermocline. The effect of fossilization or the approach to fossilization on the shape of the viscous-convective spectrum is as yet unknown.

On a variance-preserving plot (Figure 7), the low wave number difference appears less pronounced, and differences near the peak are accentuated. The high Cox number spectrum is significantly higher than the Batchelor spectrum near the peak; we attribute this to a violation of Taylor's hypothesis caused by a larger turbulent intensity for the high Cox number spectra [*Lumley*, 1965]. The first-order correction for this effect depends on the turbulent intensity and is particu-

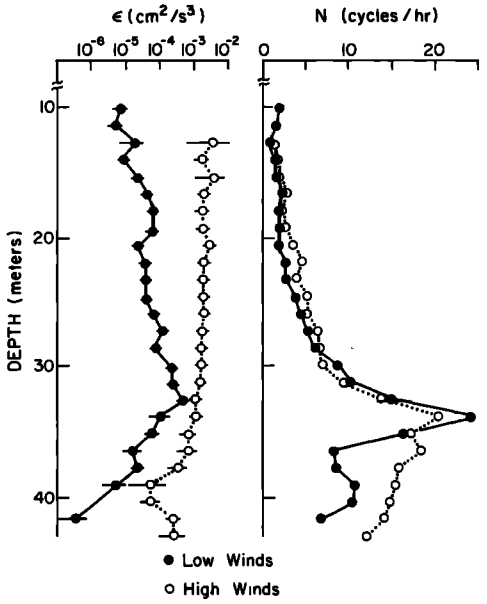


Fig. 10. Average of $\epsilon_B$ and buoyancy frequency in low (solid circle) and high (open circle) wind speed. During low winds, $\epsilon_B$ increases with depth until the thermocline is reached and shows two regions of high dissipation associated with the top of the transition zone near 20 m and the top of the thermocline at 33 m. During high winds, $\epsilon_B$ is nearly constant with depth and is much larger than during low winds. The volume average of $\epsilon_B$ should not be attempted below 30 m.

larly simple for the Batchelor spectrum, but since we do not measure the turbulent intensity, we can make no correction for this effect.

## Dissipation Rates

Dissipation rates in the surface layer and upper thermocline were estimated from the spectra by using $q = 2(3)^{1/2}$. In the early, quiet cases the dissipation rate profile was intermittent in the vertical and showed a definite increase with depth as the thermocline was approached (Figure 8). This may reflect increased shear production in the mixed layer–thermocline transition region. In the region of maximum temperature gradient the dissipation decreases and is even more intermittent and smaller below.

As the wind speed increased, the dissipation rate became larger and more uniform in the vertical (Figure 9). Again, a sharp falloff occurred where the temperature gradient was largest, but in this zone and below, the dissipation rate was significantly larger than it was earlier.

Much of the scatter due to intermittency was removed from the dissipation rate profiles by averaging all profiles from similar wind conditions (Figure 10); the depth for each cast was normalized to the 10° C isotherm to minimize the effect of internal waves. The low-wind profile shows a definite trend toward increasing dissipation with depth above the thermocline, with small peaks of dissipation both at the top and bottom of the transition zone; this may be indicative of two distinct shear zones. In the seasonal thermocline and below, the dissipation rate is severely attenuated. In contrast, the later high-wind profile average is nearly constant with depth. No intensification is seen in the transition layer, and stratification above the seasonal thermocline has no observable effect upon the profile. In addition, dissipations are larger during high winds than during low winds. We conclude that the responses of the turbulence to surface forcing is very rapid.

In modeling the surface mixed layer it is usually assumed that both the energy available for mixing and the dissipation are proportional to the cube of the wind speed [*Niiler and Kraus*, 1977]. The 'high' winds have about 3 times the speed of the 'low' winds, so the energy available for mixing is expected to increase by a factor of about 30. The calculated increase in dissipation is of approximately this magnitude. A more detailed comparison of the variation of dissipation with wind speed is not warranted from these data because the surface wave zone, in which dissipation is expected to be largest, is not adequately sampled. For this reason a depth-integrated dissipation cannot be calculated and related to changing wind stress.

The method used to calculate the mean profiles was to average all resolved dissipations during low or high winds; those cases where the spectrum was unresolvable due to any cause were not included in the average. The spectra were almost always resolved above the seasonal thermocline, so lack of resolution had little effect in the surface layer and the transition zone. However, the thermocline spectra were often unresolvable, usually because no turbulence was found sufficiently intense to produce a microstructure peak significantly above the fine structure background. Thus the profile averages below 35 m are biased toward larger values, so that dissipation rates in the thermocline region may not be representative of the actual volume average thermocline dissipation. The average of the resolved spectra in the thermocline is, however, significantly greater in high winds than in low winds, indicating that when turbulence is found in the upper seasonal thermocline, it is more intense in high winds than in low. This indication must, however, be treated rather more cautiously than conclusions regarding the mixed layer and transition zones.

One is then led to inquire how energy is transmitted through the zones of large stratification typical of the seasonal thermocline. While only speculations may be offered, two mechanisms are possible: (1) intense shearing within the thermocline and (2) transmission through the stratification by internal waves. Of these, the latter seems more plausible, because classical mean shearing implies an exchange of momentum by actual mass transport, which would cause a more continuous distribution of turbulence, while transmission by internal waves generated at the top of the thermocline requires no mass exchange. If energy leakage by internal waves through the transition zone to an already saturated internal wave field were to occur, internal wave instabilities would release energy in the thermocline region in a necessarily patchy and highly intermittent distribution. It should be noted that the two mechanisms are not mutually exclusive, for shearing of the mean flow can intensify internal wave instabilities.

A significant difference between the storm studied here and the first, stronger storm during the Mile experiment is that during this second storm, no large-scale catastrophic mixing was observed. The temperature inversions observed here were all of moderate size (~1-m vertical scale or less), while in the first Mile storm on Julian dates 235–236, larger-scale events may have been the dominant mechanism of heat and mass transport [*Dillon and Caldwell*, 1978].

## Sources of Error

The sources of error in computing the dissipation rate $\epsilon_B$ from the cutoff wave number are both random and systematic. The random error associated with determining the cutoff frequency from the spectral estimates is 5–10%, negligible

when compared with either systematic errors or the variability found in the upper waters. Another random error, associated with violation of Taylor's hypothesis due to possibly large turbulent intensity [*Lumley*, 1965], may cause a 40% overestimate of $\epsilon_B$ for intense turbulence. Surface wave orbital velocity may also introduce an uncertainty in the estimate of $\epsilon_B$, for while the microstructure profiler responds well to vertical velocities at surface wave frequencies [*Dillon and Caldwell*, 1980], its response to a fluctuating horizontal velocity field is unknown. An imperfect response would cause fluctuations in the angle of attack of the sensor and deviations from the constant value assumed for application of the Taylor hypothesis (T. R. Osborn, personal communication, 1979). Systematic error in all estimates of $\epsilon_B$ results from uncertainty in the universal constant $q$. While this does not affect comparisons of the dissipation (Figure 9), it may be the major source of error in computing volume averages of the total mixed layer dissipation.

Another source of error pertinent to volume averages lies in the fact that an estimate of $\epsilon_B$ in intermittent turbulence is biased toward the larger values. This may be seen by considering the extreme hypothetical case of a 60-cm segment which contains a turbulent core with a vertical scale of a few centimeters surrounded by nonturbulent water. In this case the turbulent core would completely determine the cutoff wave number, but an $\epsilon_B$ computed from this should not be taken as being typical of the entire 60-cm segment. An attempt to delineate such regions of turbulent and nonturbulent fluid within a segment would be a painstaking and highly subjective task, possibly subject to interpretational errors as severe as imputing the single value of $\epsilon_B$ to the entire segment. Such circumstances may occur in the seasonal thermocline, so that caution should be used in volume averaging in highly stratified and intermittent regions.

Since most of these uncertainties are impossible to assess at this time, we choose to place no error estimate on $\epsilon_B$ and simply caution the reader that large uncertainties exist. It should be noted, however, that the conclusions of this study are based upon vertical variations in $\epsilon_B$ of an order of magnitude or more and so are independent of the above uncertainties.

## CONCLUSIONS

1. The observed viscous-convective subrange spectrum of temperature gradients approaches the Batchelor spectrum as the Cox number increases. For low Cox number the spectrum is broader and flatter than the Batchelor spectrum.

2. Kinetic energy dissipation rate profiles as inferred from the spectral cutoff wave number are highly intermittent, and values grow larger with increasing wind. The response to surface forcing occurs on time scales comparable to the time scales of the forcing.

*Acknowledgments.* We thank P. A. Newberger, M. Matsler, and A. Robinson for their aid in collecting these data; S. Wilcox for constructing the electronic elements of the probe; and S. Blood for computational aid. M. C. Gregg generously provided us with preliminary results of a thermistor frequency response test of the P-85 which substantially agreed with our own. This work was supported by the Office of Naval Research, contract N00014-76-C-0067.

## REFERENCES

Batchelor, G. K., Small-scale variation of convected quantities like temperature in turbulent fluid, *J. Fluid Mech., 5,* 113–133, 1959.

Caldwell, D. R., F. E. Snodgrass, and M. H. Wimbush, Sensors in the deep sea, *Phys. Today, 22*(7), 34–42, 1969.

Caldwell, D. R., S. D. Wilcox, and M. Matsler, A relatively simple freely-falling probe for small-scale temperature gradients, *Limnol. Oceanogr., 20,* 1035–1047, 1975.

Caldwell, D. R., T. M. Dillon, J. M. Brubaker, P. A. Newberger, and C. A. Paulson, The scaling of vertical temperature gradient spectra, *J. Geophys. Res., 85,* this issue, 1980.

Dillon, T. M., and D. R. Caldwell, Temperature microstructure profiles at ocean station P: Preliminary results from the Mile experiment, *Ref. 77-22,* 215 pp., Sch. of Oceanogr., Oreg. State Univ., Corvallis, 1977.

Dillon, T. M., and D. R. Caldwell, Catastrophic events in a surface mixed layer, *Nature, 276,* 601–602, 1978.

Dillon, T. M., and D. R. Caldwell, High-frequency internal waves at ocean station P, *J. Geophys. Res., 85,* in press, 1980.

Elliott, J. A., and N. S. Oakey, Spectrum of small-scale oceanic temperature gradients, *J. Fish. Res. Bd. Can., 33,* 2296–2306, 1976.

Fabula, A. G., The dynamic response of towed thermistors, *J. Fluid Mech., 34,* 449–464, 1968.

Gibson, C. H., Finestructure of scalar fields mixed by turbulence, 1, 2, *Phys. Fluids, 11,* 2305–2327, 1968.

Gibson, C. H., and W. H. Schwarz, The universal equilibrium spectra of turbulent velocity and scalar fields, *J. Fluid Mech., 16,* 365–384, 1963.

Gibson, C. H., R. R. Lyon, and I. Hirschsohn, Reaction product fluctuations in a sphere wake, *AIAA J., 8,* 1859–1863, 1970.

Grant, H. L., B. A. Hughes, N. M. Vogel, and A. Moilliet, The spectrum of temperature fluctuations in turbulent flow, *J. Fluid Mech., 34,* 423–442, 1968.

Gregg, M. C., Finestructure and microstructure observations during the passage of a mild storm, *J. Phys. Oceanogr., 6,* 528–555, 1976.

Gregg, M. C., Variations in the intensity of small-scale mixing in the main thermocline, *J. Phys. Oceanogr., 7,* 436–454, 1977.

Lumley, J. L., Interpretation of time spectra measured in high-intensity shear flows, *Phys. Fluids, 8*(6), 1056, 1965.

Marmorino, G. O., and D. R. Caldwell, Temperature finestructure and microstructure observations in a coastal upwelling region during a period of variable winds (Oregon, summer 1974), *Deep Sea Res., 25,* 1073–1106, 1978.

Nasmyth, P. W., Oceanic turbulence, Ph.D. thesis, 69 pp., Inst. of Oceanogr., Univ. of B. C., Vancouver, 1970.

Niiler, P. P., and E. B. Kraus, One dimensional models of the upper ocean, in *Modelling and Prediction of the Upper Layers of the Ocean,* edited by E. B. Kraus, Pergamon, New York, 1977.

Otnes, R. K., and L. Enochson, *Digital Time Series Analysis,* 467 pp., John Wiley, New York, 1972.

Schedvin, J. C., Microscale measurements of temperature in the upper ocean from a towed body, Ph.D. thesis, Univ. of Calif. at San Diego, La Jolla, 1979.

Tennekes, H., and J. L. Lumley, *A First Course in Turbulence,* 300 pp., MIT Press, Cambridge, Mass., 1972.

Turner, J. S., *Buoyancy Effects in Fluids,* 367 pp., Cambridge University Press, New York, 1973.

Williams, R. M., and C. A. Paulson, Microscale temperature and velocity spectra in the atmospheric boundary layer, *J. Fluid Mech., 82,* 547–567, 1977.

(Received June 20, 1979;
revised November 5, 1979;
accepted November 15, 1979.)